Progress In Electromagnetics Research M, Vol. 111, 13–25, 2022

A Small Disk-Coupled Circularly Polarized Microstrip Ring Antenna for Microwave Energy Harvesting

Cheng Peng[1, 2], Zhi-Hao Ye[1], Han Xiao[1, *], Jing Huang[1], Ning-Zhao Luo[1], and Dong Wu[2]

Abstract—A small ring antenna working at 2.45 GHz was designed in this paper, a small disk-coupled structure was applied to feed an inner-hole-biased ring patch, contributing to not only improving the impedance characteristics of the antenna but also reducing the size. The simulation results show that the designed patch area is only 70.7% of that of the traditional circular microstrip antenna on the premise of ensuring good bandwidth and gain performance; the −10 dB bandwidth of S_{11} parameter is 62 MHz; the gain of the maximum direction is 7.11 dB; and the circular polarization of the antenna is also realized. This design has also been compared with several conventional designs. It is proved that the antenna has good comprehensive performance, and the antenna feed structure is simple, easy to process, very conducive to engineering applications. Finally, the feasibility of this technology was verified by contrasting the measured data with the simulation data.

1. INTRODUCTION

With the advancement of technology, the applications of antenna are more and more diversified, such as the development of wireless power transmission technology in recent years. Antennas are widely adopted in microwave wireless energy transmission (MWPT) systems, as shown in Fig. 1. The MWPT systems use microwave as an energy carrier and mainly rely on a transceiver antenna for microwave energy transmission, which accounts for the advantage of long transmission distance. This type of antenna is usually large in size and not suitable for integration in some small devices. In order to balance size and efficiency, space-focused transfer technology has been used in MWPT systems. The focus-transfer technology can concentrate the beam. Increasing the power density per unit area makes it possible for small RF energy receiving antennas [1], so miniaturization should be favored, which has been a topic worth studying. In addition to miniaturization, the stability of energy harvesting must also be considered. A microwave rectifier circuit at the receiving end is only under specific power input peak efficiency [2] so that the input power of the receiving antenna should be steady and would not be sensitive to polarization deflection. A circularly polarized antenna can help prevent the fluctuation of the input power of the receiver, which adds to microwave energy harvesting.

At present, some research has already focused on miniaturization of the microstrip antenna. According to the basic principle of microstrip antenna, when the dielectric constant is at a certain value and the patch shape fixed, the working frequency of the antenna along with its size can be generally determined [3]. It should be noted that the antenna size is expected to be smaller for some special occasions. For instance, some references have used substrates with high dielectric constants to achieve the purpose of miniaturization. However, if dielectric plates with a high dielectric constant are directly employed, the serious surface wave effect will occur, resulting in the decrease of radiation efficiency and

Received 29 April 2022, Accepted 25 May 2022, Scheduled 14 June 2022
* Corresponding author: Han Xiao (xiaohan19890823@126.com).
[1] Naval Engineering University, Wuhan 430000, Hubei, China. [2] National University of Defense Technology, Wuhan 430010, Hubei, China.

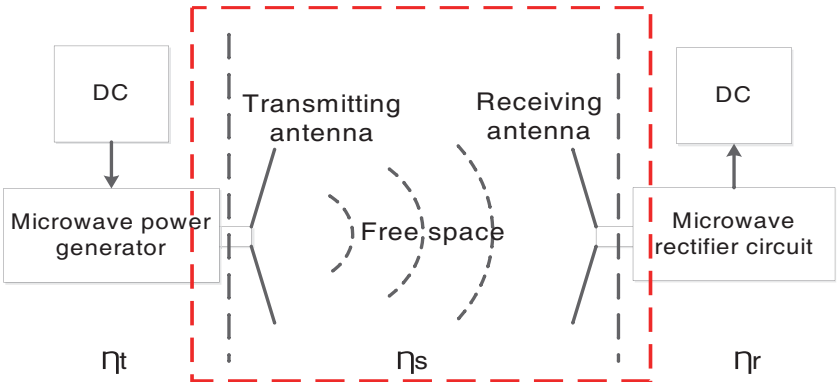

Figure 1. MWPT system diagram.

thus affecting the gain performance of the antenna [4–6]. Some scholars also dig holes on the surface of the patch. Since the current flows on the surface of the patch, it functions as introducing cascade inductance into the equivalent circuit of the antenna, so that the size of the patch will be reduced [7]. Nevertheless, the inductance introduced will deteriorate the impedance matching characteristics of the antenna and impact the antenna S_{11} parameters. Some scholars also design a small bending and folding microstrip line antenna, which is conducive to sacrificing horizontal or vertical distance to an end to weaken the antenna size. Additionally, scholars not only concentrate on the surface patch but also adopt some specialized feed ways, such as the utilization of a disk-coupled microstrip feed antenna, square ring, and ring microstrip antenna whose size is smaller than a conventional patch antenna (because it increases the current path). Given that the disk feeder can compensate for the patch surface hole inductance, impedance characteristics can be considerably improved under the circumstance. Although there is progress made in compressing the microstrip antenna, people still face challenges to pull off miniaturization and circular polarization in the same design while keeping antenna performance not worsened. On the one hand, in the design of a circularly polarized microstrip antenna, the feed network itself stands as a certain size. On the other hand, realizing the circular polarization means that miniaturization cannot be easily secured. Double-fed or multi-fed technology is the most frequently used method to realize circular polarization of a microstrip antenna. The multi-feed method can obtain better axial ratio characteristics, but the feed network is complex and large due to the application of multi-feed points. To notch up circular polarization through a single feed [8–16], it is necessary to feed in the orthogonal direction with a difference of 90 degrees to stimulate circular polarization. Due to the inductance effect on the surface of the patch, it is difficult to realize impedance matching and easy to produce machining errors. This paper is based on the asymmetric ring patch, as a ring structure can improve the surface current distribution by changing the antenna's equivalent circuit so as to realize miniaturization [16–19], and the single-fed circularly polarized antenna can be realized by bias hole on the antenna surface so as to optimize the impedance characteristics of the patch antenna fed by single disk-coupled feed, better performing the miniaturization and circular polarization effect. Considering its simple feed structure, it is more beneficial to antenna processing and engineering implementation.

2. ANTENNA DESIGN CONCEPT

2.1. Antenna Miniaturization

First and foremost, the probe fed by a circular microstrip antenna is deemed as a reference. The performance of the feed is stable, whilst the inherent size of the antenna is limited by frequency, so it cannot be miniaturized. Moreover, the probe itself has inductance characteristics, which will suppress the high frequency signal. The size and shape after simulation and optimization are shown in Fig. 2(a). For the purpose of compressing a microstrip antenna, this paper turns the original film into a ring form. In a bid to facilitate the impedance matching characteristics of the circular antenna, a disk-coupled feed was deployed to simulate a miniature circular coupling antenna, which is illustrated in Fig. 2(b).

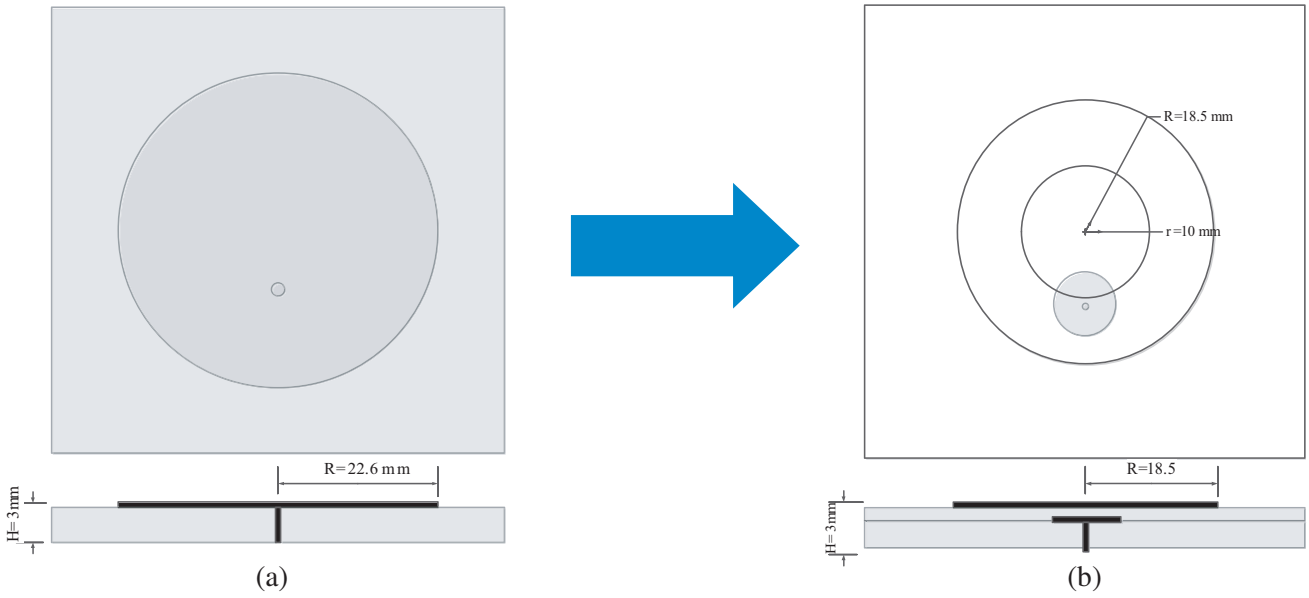

Figure 2. Antenna I/II structure diagram. (a) Antenna I structure diagram. (b) Antenna II structure diagram.

As per the theory of the microstrip antenna [20], the equivalent circuits of Antenna I and Antenna II can be portrayed. In the working state, Antenna I can be equal to a parallel circuit composed of equivalent capacitance C_{mn}, inductance L_{mn}, admittance G_{mn}, and equivalent resistance R_{mn} generated by resonant mode T_{mn}. The resonant frequency determined in this paper was 2.45 GHz. The reason for choosing this frequency is that mobile services in this frequency band are concentrated, and the space transmission loss is small, which will make for collecting more microwave energy. For probe feed, it is mainly present in inductance characteristics at 2.45 GHz, and the inductance value can be on a par with L_k, as proven in Fig. 3(a). The patch of Antenna II can also equate with a parallel circuit composed of capacitance C'_{mn}, inductance L'_{mn}, and admittance G'_{mn} in the mode T_{mn}. Yet, due to the introduction of disk coupling on the feed probe for capacitive impedance compensation, the equivalent parameters during feeding can be equal to inductance L'_k and capacitance C'_k in series. The identical circuit is plotted in Fig. 3(b).

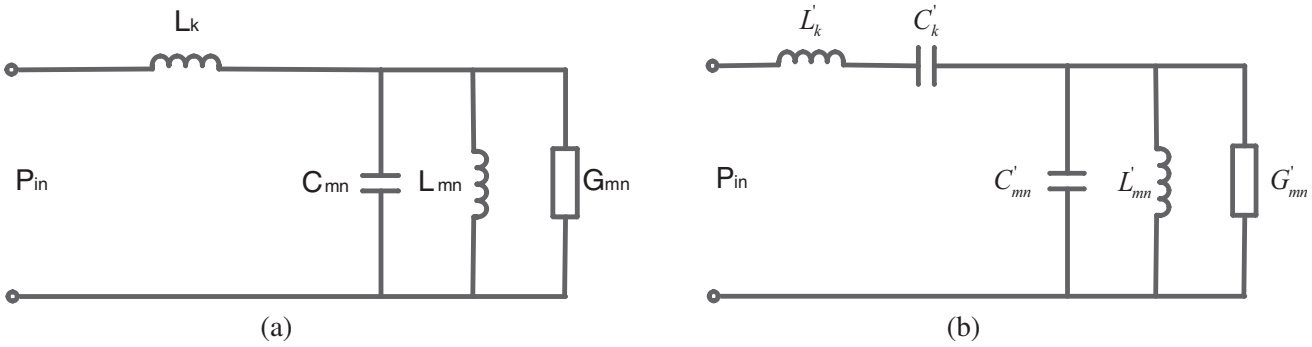

Figure 3. Antenna I/II equivalent circuit model. (a) Equivalent circuit of antenna I. (b) Equivalent circuit of antenna II.

Based on the equivalent circuit parameters of the microstrip antenna and the related theory of the microstrip antenna [20, 21], the antenna quality factor Q and bandwidth BW can be figured out. It can be seen from formula (2) that the bandwidth BW is inversely proportional to the quality factor Q, and

the quality factor Q is subject to the resistance R_{mn}, inductance L_{mn}, and capacitance C_{mn} generated under the mode T_{mn}. When the working frequency of the antenna is identified, these factors are only associated with the inherent size, shape, and material of the antenna.

$$C_{mn}Q = R_{mn}/\sqrt{L_{mn}/C_{mn}} \tag{1}$$

$$BW = \frac{\rho - 1}{\sqrt{\rho}Q} \times 100\% \tag{2}$$

For the circular form of antenna II, owing to the inductive effect of the surface caused by the extension of the current path, there is $L'_{mn} > L_{mn}$, while the patch size will decline, resulting in $C'_{mn} < C_{mn}$. According to the LC equivalent circuit frequency calculation formula, it can be shown that the design of antenna II is able to trim the resonant frequency better than Antenna I when registering antenna miniaturization. On the other hand, at the same resonant frequency, such a design can also reduce the size of the antenna:

$$\omega_{mn}(\mathrm{II}) = 1/\sqrt{L'_{mn}/C'_{mn}} < \omega_{mn}(\mathrm{I}) = 1/\sqrt{L_{mn}/C_{mn}} \tag{3}$$

The antenna I/II model is established on the simulation software, as shown in Fig. 4. Parameters are tuned in two types of antennas, leading to two types with different size parameters. The operating frequencies of Antenna I and Antenna II are at 2.45 GHz, with dielectric constant ε_r 2.2, thickness H 3 mm, the positions of feed point 6.5 mm and 6.4 mm from the distance d at the center, respectively, and the radii of Antenna I and Antenna II 22.6 mm and 18.5 mm, respectively. Besides, antenna II has two layers; the thickness of the upper layer is $H_1 = 1$ mm; the thickness of the lower layer is $H_2 = 2$ mm; the radius of the inner hole $r = 10$ mm; the feeding disc radius $s = 5$ mm; and the parameters of each type are listed in Table 1.

Table 1. Antenna I/II parameter list.

Antenna	R	r	H	$H1$	$H2$	d	S	ε_r
I	22.6 mm	-	3 mm			6.5 mm	-	2.2
II	18.5 mm	10 mm	3 mm	1 mm	2 mm	6.4 mm	5 mm	2.2

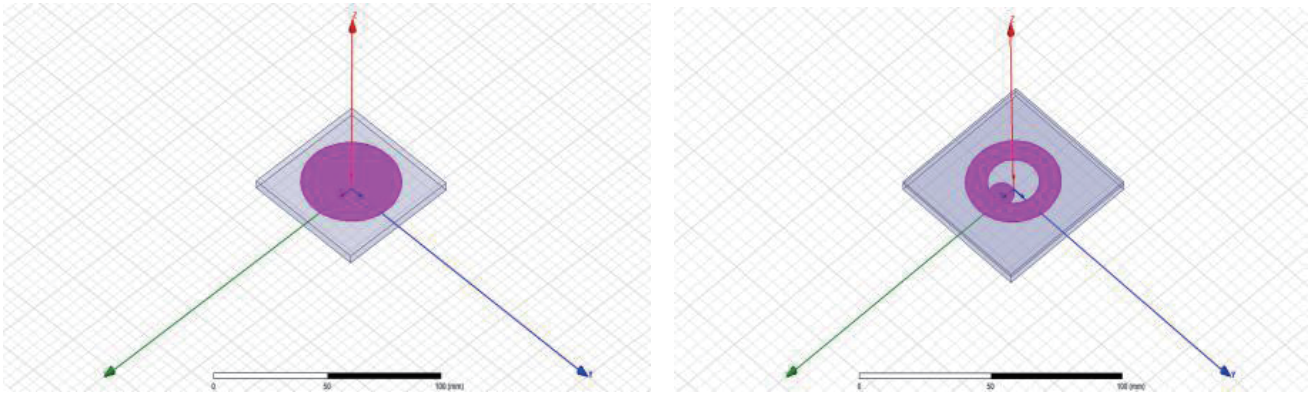

Figure 4. The simulation model of Antenna I/II.

The S-parameters and gain of the simulated Antenna I/II are compared as shown in Fig. 5. It can be observed from the simulation that the S_{11} parameter of Antenna I is $S_{11} < -38$ dB at the center, and its -10 dB bandwidth can reach 70 MHz, while $S_{11} < -25$ dB bandwidth at the center frequency of Antenna II after miniaturization design is only 38 MHz. It can be fathomed from Formulas (1) and (2) that this can be attributed to the increase of the Q value on account of the change of antenna size and shape, entailing the reduction of the antenna bandwidth. The gain performances of the two

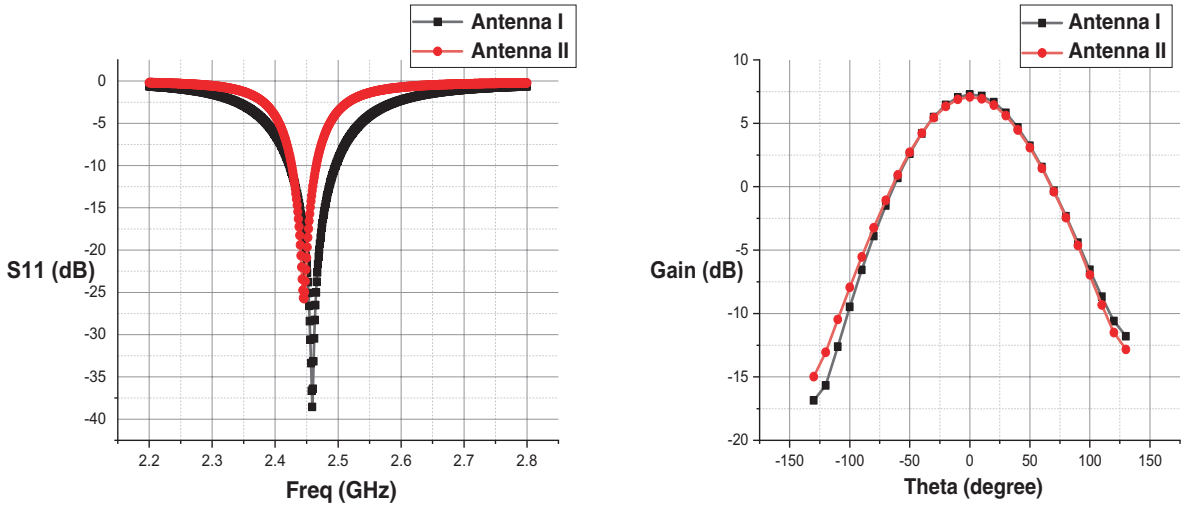

(a) (b)

Figure 5. Antenna I/II S_{11} and gain comparison. (a) S_{11} comparison. (b) Gain comparison.

antennas are close to each other, and the maximum radiation direction is over 7 dB. The simulation results indicate that the design reduces the patch radius to 18.5 mm without changing the frequency, gain, dielectric plate thickness, and materials. Although the antenna bandwidth is affected, it is still working at 2.45 GHz, and the patch area of Antenna II accounts for only 67% of that of Antenna I, bringing an excellent miniaturization effect.

Although antenna II adopts the disk coupling feed for capacitor compensation, it can be seen from the parameters of S_{11} that its impedance characteristics are still not as ideal as antenna I. According to the equivalent circuit and microstrip antenna related theories as shown in Fig. 3 [7], we can obtain the impedance calculation formulas of antenna I and antenna II:

$$Z_{in} = \frac{1}{G_{mn} + j\left(\omega C_{mn} - \dfrac{1}{\omega L_{mn}}\right)} + j\omega L_k = \frac{1}{\dfrac{1}{R_{mn}} + j\left(\omega C_{mn} - \dfrac{1}{\omega L_{mn}}\right)} + j\omega L_k \tag{4}$$

$$Z'_{in} = \frac{1}{\dfrac{1}{R'_{mn}} + j\left(\omega C'_{mn} - \dfrac{1}{\omega L'_{mn}}\right)} + j\left(\omega L'_k - \frac{1}{\omega C'_k}\right) \tag{5}$$

2.2. Antenna Circular Polarization

Compared with antenna I, antenna II achieves miniaturization by changing the equivalent circuit structure of antenna, but it is difficult to achieve both the miniaturization and circular polarization on the premise of guaranteeing the performance of antenna. Though double-feed or multi-feed is the most commonly used method to realize circular polarization of micro-strip antenna at present, the feeding network itself has a certain size and needs to be designed independently. Although circular polarization can be realized by double-fed or multi-fed methods, the antenna structure is complicated and huge due to the application of multi-fed technology, which requires additional feed network. Different from the multi-feed technology, the single-feed circular polarization only needs one feed point to feed the antenna, and there is no need to design additional complex power distribution feed circuit and phase shifting network. The simple structure is more convenient for miniaturization and engineering implementation. The principle of circular polarization realized by single feeders is similar to that of double feeders, which requires constant amplitude excitation with a difference of 90 degrees in the orthogonal direction. The difference is that it is difficult for the patch with regular shape to get the degenerated mode (TM_{01}, TM_{10}) with a difference of 90 degrees by a single feeder, and the perturbation element ΔS needs to be added in the orthogonal direction.

Figure 6. Antenna circular polarization design concept. (a) Antenna II structure diagram. (b) Antenna III structure diagram.

In order to realize circular polarization, the circular polarization of antenna II is improved by adding degenerate element ΔS, and single feed is adopted to simplify the feed network. In the design, the inner hole of antenna II is offset, and antenna III was designed. The disk coupling feed was continued, as shown in Fig. 6. TM_{01} and TM_{10} modes are excited in the orthogonal direction of the patch surface by such an asymmetric structure. The polarizations of the two main modes are orthogonal. When the perturbation element S is appropriate, and the direction of the electric field rotates along a circular orbit with the direction of propagation as its axis. The difficulty in the design of a circularly polarized microstrip antenna fed by a single point lies in the reasonable design of the size and position of the perturbation element and the position of the feed point. When both modes are resonant at 2.45, circularly polarized radiation is achieved at that frequency point.

3. ANTENNA DESIGN AND SIMULATION

3.1. Antenna Structure and Dimensions

Through the design of miniaturization and circular polarization and ultimately determining antenna III structure diagram as shown in Fig. 7, the antenna still uses the dielectric constant of 2.2 medium plate; the shape of the sheet is a square with sides of length a; the total thickness of the antenna is H with upper medium plate thickness of h_1, the thickness of the medium plate below for h_2, the circular patch radius R, and the internal hole radius r. The distance between the feed point and the center is d_1. The offset distance of the inner hole is d_2, and the radius of the feed disk is S. The antenna size parameters are optimized on the electromagnetic simulation software, as shown in Fig. 8. When the antenna center frequency is 2.45 GHz, the ANTENNA S parameter, gain, and axis ratio are optimized as far as possible. The parameter of antenna III is shown in Table 2.

Table 2. Parameter list of antenna III.

Antenna	ε_r	a	H	$h1$	$h2$	R	r	$d1$	$d2$	s
III	2.2	60 mm	3 mm	1 mm	2 mm	19 mm	10.25 mm	6.1 mm	2.7 mm	4.9 mm

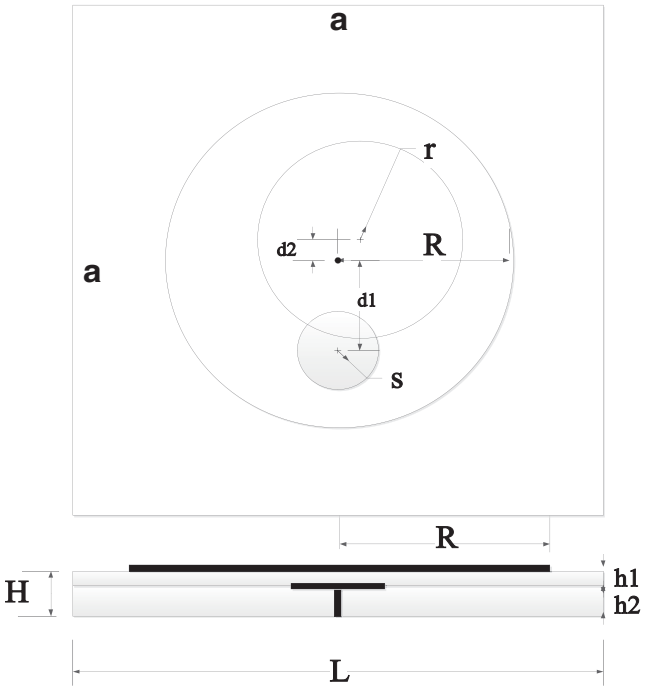

Figure 7. Structure diagram of Antenna III.

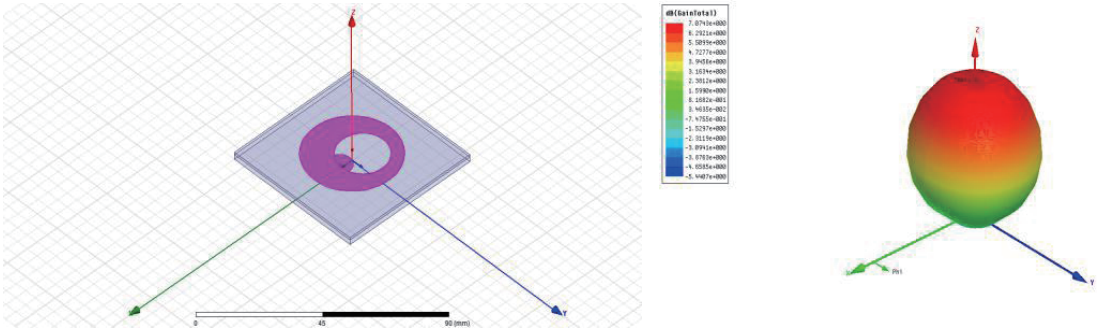

Figure 8. The simulation model of Antenna III.

Similarly, antenna III also operates at 2.45 GHz. The patch radius of antenna III is $R = 19$ mm, which is close to the patch radius of antenna II of 18.5 mm, indicating that antenna III inherits and maintains the miniaturization effect of antenna II well, and by calculation, the patch area of antenna III is only 70.7% of that of antenna I at the same operating frequency, achieving good miniaturization effect. Antenna III can also form degenerate mode ΔS unit so as to realize circular polarization.

3.2. Antenna Simulation Results

The S_{11}-freq curve of the designed antenna III is obtained through simulation, and the S_{11} curves of antenna III and antenna I are compared and analyzed, as shown in Fig. 9. As can be seen from the figure, the bandwidth of antenna III is almost unchanged from that of antenna I, the bandwidth of -10 dB only 10 MHz less, and the gain performance almost unchanged. It shows that the improved design has little effect on the bandwidth of the antenna and does not affect the normal operation of the antenna.

Similarly, the far field of the antenna is simulated on the simulation software, and the gain directions of E-plane and H-plane of antenna III are obtained, as shown in Fig. 10(a) and Fig. 10(b). Gain is

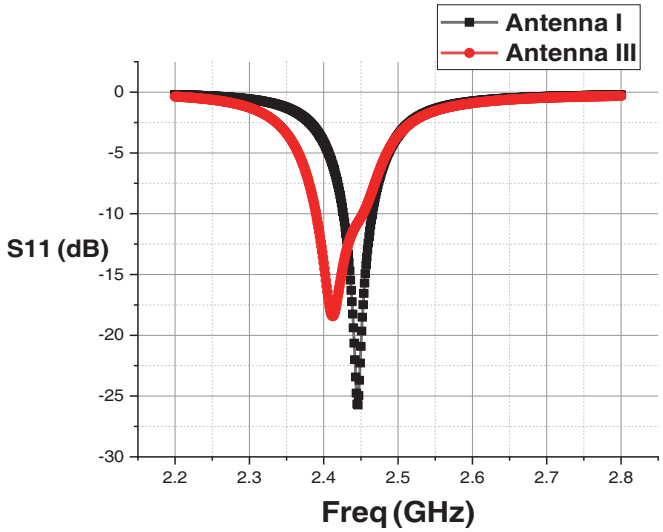

Figure 9. S_{11} curve contrast of antenna I/III.

the product of directivity coefficient and efficiency, which can objectively reflect the antenna's ability to receive microwave energy [22, 23]. It can be seen from the figure that the antenna has almost no side-lobe radiation and backward radiation. The direction with the strongest receiving ability is concentrated in the forward direction, and the gain of the maximum radiation direction (Phi = 0°) reaches 7.11 dB. This shows that the antenna has a good ability to receive microwave energy in the maximum radiation direction, and no matter E plane or H plane of antenna III, the 3 dB beam width is wider than 80 degrees, and the 0 dB beam width is wider than 140 dB. The E and H plane direction figures are roughly consistent, which shows that the radiation direction of the antenna is uniform and symmetrical.

The axial ratio characteristics of the antenna in the far field are simulated, shown in Fig. 11. After optimization, the maximum axial ratio of the antenna in the direction of radiation is 2.13 dB, and the axial ratio in the range of 170 degrees of beam width is less than 3 dB, no matter in plane E or in plane H. This indicates that the circular polarization of the antenna is well realized in almost the whole main lobe direction (forward).

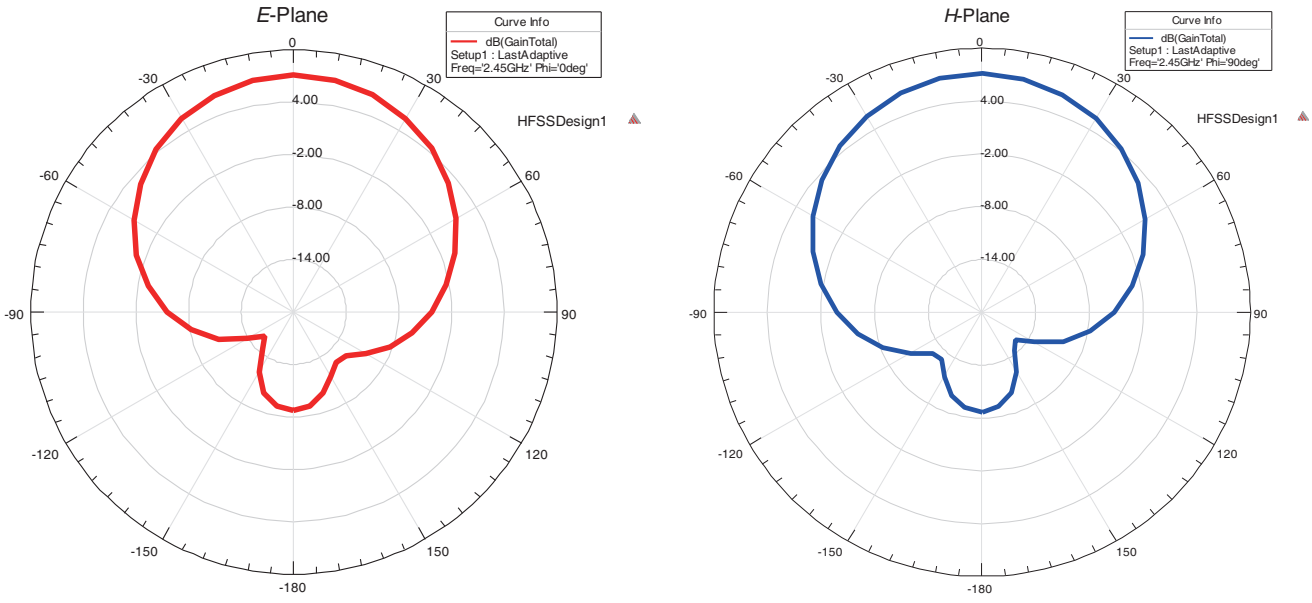

(a) (b)

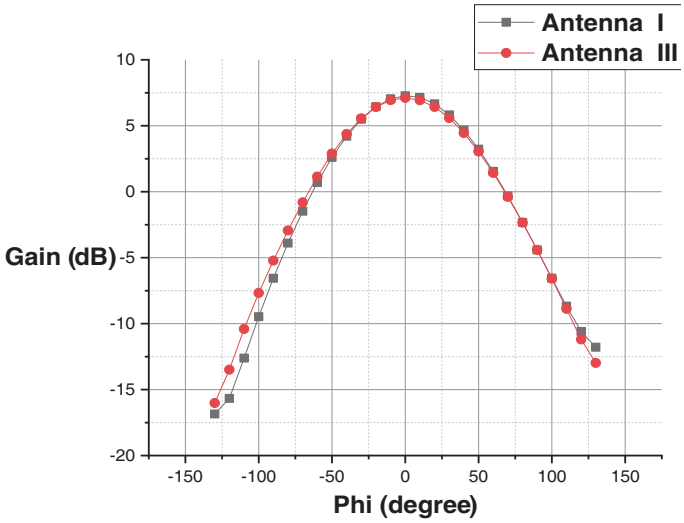

(c)

Figure 10. Simulation of antenna III gain pattern. (a) Gain of plane E. (b) Gain of plane H. (c) Gain of plane E.

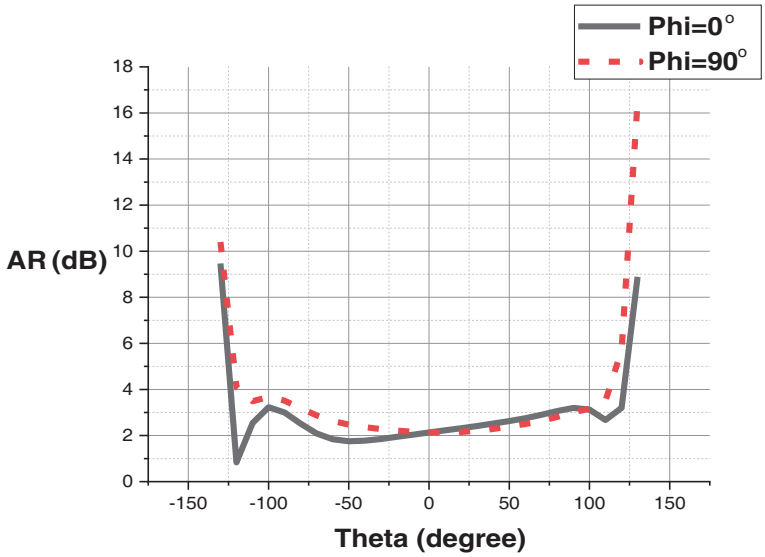

Figure 11. Simulation of axial ratio beamwidth of antenna III.

3.3. Comparison between Simulation and Measured Data

Antenna III was fabricated and tested, as shown in Fig. 12. The simulation results of antenna III are compared with the measured ones. A microwave darkroom was selected for measuring data in the experiment. The standard horn antenna was leveraged at the transmitting end, and the designed antenna was placed at the receiving end. The maximum radiation direction of the antenna was co-axial with the standard horn antenna and oriented towards the standard horn antenna. The field intensity measured at different angles is contrasted with the standard horn antenna in an end to obtain the gain direction diagram of the antenna. When measuring the axis ratio, the antenna under test was fixed, then the transmitting antenna angle was rotated from -130 degrees to $+130$ degrees along with *Phi* angle, and then the amplitude difference under different angles was measured and compared with the standard value. From the measured data in Fig. 12, the measured results are basically consistent with the simulation ones despite certain small differences, which are mainly attributed to errors related to

(a) (b) (c)

Figure 12. Antenna and test environment. (a) Antenna object. (b) S-parameter measurement. (c) Microwave dark room.

the machine, material, and measurement, certifying the feasibility of the design.

As shown in the simulation curve in Fig. 13(a), the center frequency of the antenna is about 2.45 GHz; S_{11} is −18.44 dB at the center frequency; the bandwidth of −10 dB can reach 60 MHz; and the bandwidth of −15 dB stands at around 25 MHz, which is wide enough for energy transmission. It can be clearly observed from the rectangular coordinate diagram of gain in Fig. 13(b) that the maximum gain can achieve 7.11 dB when Theta is 0 degrees while the 3 dB beam width of the microstrip antenna designed in this paper exceeds 80 degrees, and the gain is still greater than 0 dB when Theta reaches 140 degrees, signifying that the design has a favorable beam width and can adapt to all sorts of application scenarios. The axial ratio characteristics of the simulated antenna are portrayed in Fig. 13(c). It can be noted that the axial ratio of the antenna is less than 3 dB in the radiation range of 170 degrees, suggesting that the antenna has a good axial ratio beam width which indicated that the antenna can accommodate to different E-field direction. The design of antenna III is compared with some similar designs in literature, as shown in Table 3. In this paper, some miniaturized microstrip antennas with frequencies close to 2.45 GHz are selected for comparison.

It can be drawn from Table 3 that the miniaturization effect of the designed antenna III is close to that of the linearly polarized antenna and even outperforms that of some circularly polarized antennas. The design of antenna III is relatively simple in structure, convenient in fabrication, and registers good gain effect, indicating that the design has comprehensive performance advantages, and such a small and comprehensive antenna, working in the 2.45 GHz band, is very suitable for wireless charging of small wearable devices.

Table 3. Comparison with similar design.

References	Frequency	Gain ($\theta = 0$)	Polarization	Size reduction (area)
[24]	2.4 GHz	-	LP	31.8%
[25]	2.4 GHz	-	LP	31%
[26]	2.4 GHz	3 dB	LP	33%
[27]	2.4 GHz	4.88 dB	LP	22%
[28]	2.45 GHz	2.9 dB	CP	10.4%
[3]	1.575 GHz	3 dB	CP	23.4%
Antenna III	2.45 GHz	7.11 dB	CP	29.3%

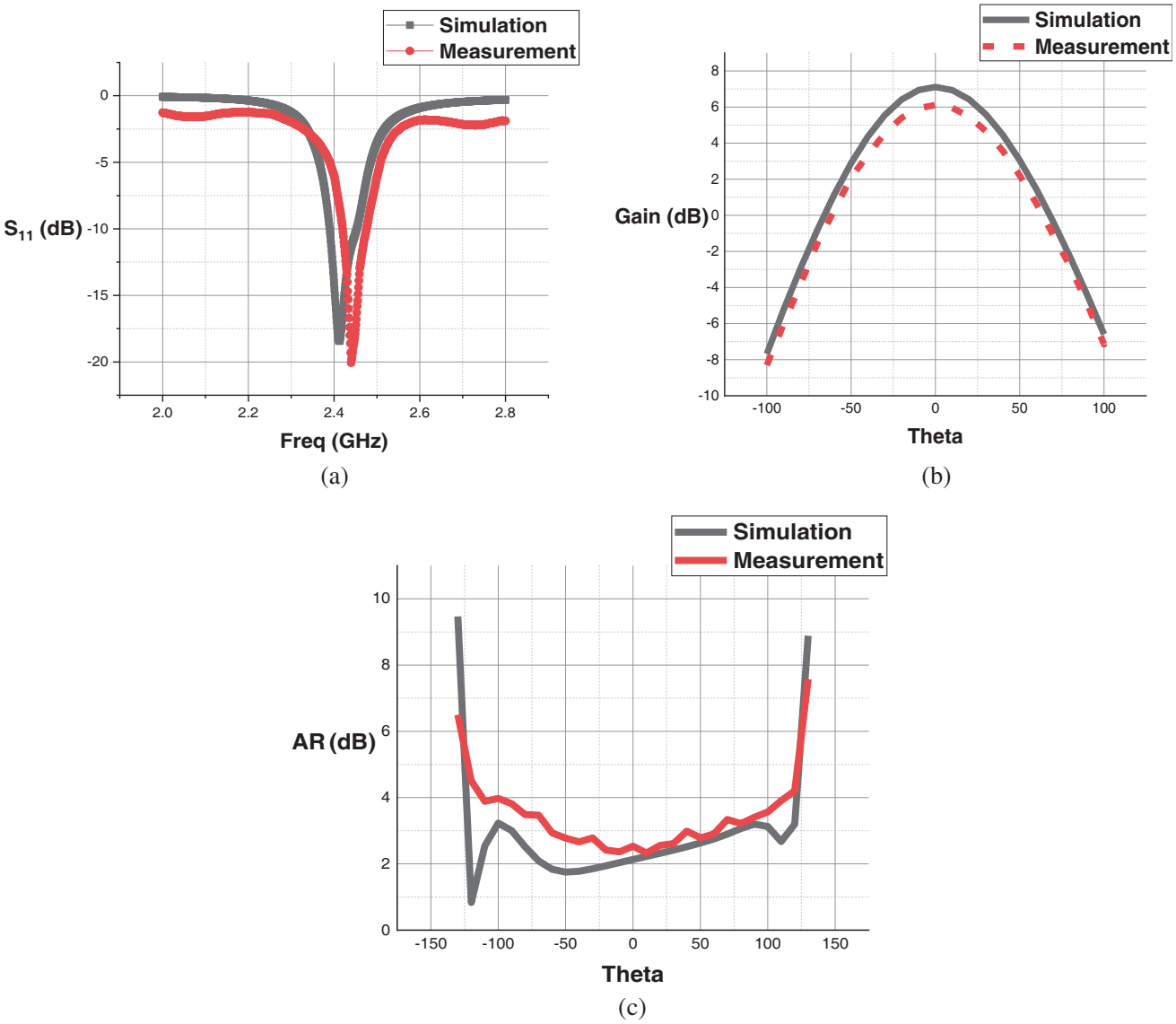

Figure 13. Comparison of antenna III simulation and measured data. (a) S_{11} comparison. (b) Gain comparation. (c) Axial ratio comparison.

4. CONCLUSION

In this paper, a circular microstrip antenna based on disk-coupled feed has been designed. By leaving a circular offset hole on the surface of the circular patch, the simulation denoted that without changing the antenna gain, the patch size was pruned to 70.7% of the traditional form; the maximum radiation direction axial ratio was 2.1 dB; the maximum radiation direction gain of the antenna is 7.11 dB; and -10 dB bandwidth of S_{11} parameter is 62 MHz. By comparing several traditional designs, a conclusion is drawn that the antenna structure holds a significant advantage, that is, achieving circular polarization while realizing a good miniaturization effect. Moreover, this structure is also equipped with the advantages of a simple feeding network and easy processing. Upon processing and actual measurement, the conclusion of this paper was thus verified. Such advantages make the antenna suitable for small devices for microwave energy harvesting. The next step is to add the antenna to a wearable device, with a rectifier on the back end, for some practical testing.

REFERENCES

1. Peng, C., Z.-H. Ye, Y.-H. Xia, and C. Yang, "Analysis on space transmission model of the Microwave Wireless Power Transfer system," *Frequenz*, Vol. 75, 449–458, 2021.
2. Xiao, Y. Y., Z.-X. Du, and X. Y. Zhang, "High-efficiency rectifier with wide input power range based on power recycling," *IEEE Transactions on Circuits and Systems II: Express Briefs*, Vol. 65, 744–748, 2018.
3. Peng, C., T. Yu, H. Li, and W. Cao, "Research on circularly polarized small disk coupled square ring microstrip antenna for GPS application," *2013 Proceedings of the International Symposium on Antennas & Propagation*, Vol. 01, 380–383, Nanjing, China, 2013.
4. Mehrparvar, M. and F. H. Kashani, "Microstrip antenna miniaturization using metamaterial structures," *20th Iranian Conference on Electrical Engineering (ICEE2012)*, 1243–1246, Tehran, Iran, 2012.
5. Ding, K., T. Yu, D.-X. Qu, and C. Peng, "A novel loop-like monopole antenna with dual-band circular polarization," *Progress In Electromagnetics Research C*, Vol. 45, 179–190, 2013.
6. Ding, K., T. B. Yu, D. F. Guan, and C. Peng, "Stacked tri-band circularly polarized microstrip patch antenna for CNSS applications," *Applied Mechanics and Materials*, Vol. 347, 1786–1789, 2013.
7. Alaukally, M., T. A. Elwi, and D. C. Atilla, "Miniaturized flexible metamaterial antenna of circularly polarized high gain-bandwidth product for radio frequency energy harvesting," *International Journal of Communication Systems*, 2021.
8. Wong, K.-L. and J.-Y. Wu, "Single-feed small circular polarized square microstrip antenna," *Electronic Letters*, Vol. 5, 45–46, 1997.
9. Han, Y. and D. Su, "Design of circularly polarized GPS microstrip antenna with single-feed point," *Electronic Measurement Technique*, Vol. 11, 50–55, 2006.
10. Yang, L., L. J. Xu, Y. M. Bo, and M. Zhang, "A single-feed dual-band circularly polarized microstrip antenna with spiral slots," *2017 International Applied Computational Electromagnetics Society Symposium (ACES)*, 1–2, Suzhou, China, 2017.
11. Zhang, J., "*Microstrip Antenna Theory and Engineering*, National Defense Industry Press, Beijing, 1988.
12. Li, H., S. Fang, and W. Ding, "Low cost high gain microstrip antenna design," *Proceedings of the National Antenna Annual Conference 2010*, 45–50, Beijing, 2010.
13. Carrez, F. and J. Vindevoghel, "Experimental study of an integrated linear array microstrip antenna for monolithic fabrication," *Microwave and Optical Technology Letters*, Vol. 16, 233–236, 1997.
14. Yuwono, R. and R. Syakura, "2.4 GHz circularly polarized microstrip antenna for RFID application," *Advanced Computer and Communication Engineering Technology*, 37–42, Berlin, Heidelberg, Springer, 2015.
15. Daneshmandian, F., P. Dehkhoda, and A. Tavakoli, "A miniaturized circularly polarized microstrip antenna for GPS applications," *2014 22nd Iranian Conference on Electrical Engineering (ICEE)*, 1653–1656, 2014.
16. Elwi, T. A. and A. M. Al-Saegh, "Further realization of a flexible metamaterial-based antenna on indium nickel oxide polymerized palm fiber substrates for RF energy harvesting," *International Journal of Microwave and Wireless Technologies*, Vol. 13, No. 1, 1–9, 2020.
17. Elwi, T. A., D. A. Jassim, and H. H. Mohammed, "Novel miniaturized folded UWB microstrip antenna-based metamaterial for RF energy harvesting," *International Journal of Communication Systems*, Vol. 33, No. 6, 2020.
18. Elwi, T. A., Z. Hassain, and O. A. Tawfeeq, "Hilbert metamaterial printed antenna based on organic substrates for energy harvesting," *IET Microwaves, Antennas & Propagation*, Vol. 13, No. 12, 2185–2192, 2019.

19. Elwi, T. A., "Novel UWB printed metamaterial microstrip antenna based organic substrates for RF-energy harvesting applications," *AEU — International Journal of Electronics and Communications*, 2019.
20. Zhong, S., *Theory and Application of Microstrip Antenna*, Xidian University Press, Xi'an, 1991.
21. Zhang, R., J. Huang, J. Ding, and G. Zhai, "Compact broadband circularly polarized microstrip antenna with a cross-slotted ground plane," *2019 IEEE International Symposium on Antennas and Propagation and USNC-URSI Radio Science Meeting*, 1753–1754, Atlanta, GA, USA, 2019.
22. Almizan, H., T. A. Elwi, and Z. Hassain, "Circularly-polarized, wide-range coverage azimuth and elevation angles microstrip antenna for RF harvesting," *Journal of Engineering and Sustainable Development*, Vol. 24 (special), 191–198, 2020.
23. Almizan, H., T. A. Elwi, and Z. Hassain, "Circularly-polarized, wide-range coverage azimuth and elevation angles microstrip antenna for RF harvesting," *Journal of Engineering and Sustainable Development*, Vol. 24 (special), 191–198, 2020.
24. Meng, F. and S. K. Sharma, "A single feed dual-band (2.4 GHz/5.8 GHz) miniaturized patch antenna for Wireless Local Area Network (WLAN) Communications," *2014 XXXIth URSI General Assembly and Scientific Symposium (URSI GASS)*, 1–4, Beijing, China, 2014.
25. Meng, F. and S. Sharma, "A single feed dual-band (2.4 GHz/5 GHz) miniaturized patch antenna for Wireless Local Area Network (WLAN) communications," *Journal of Electromagnetic Waves and Applications*, Vol. 30, 2390–2401, 2016.
26. Chen, H.-R., R.-X. Che, and Y. Shao, "A compact microstrip antenna with 2.4 GHz," *Wireless Communication Technology*, Vol. 18, 30–32, 2009.
27. Chen, C., "Design of miniaturized 2.4 GHz microstrip patch antenna," *Journal of Taiyuan Normal University (Natural Science Edition)*, Vol. 13, 66–69, 2014.
28. Peng, C., T.-B. Yu, H.-B. Li, and P.-C. Xu, "Design and implementation of a novel single-feed microstrip antenna for GPS applications," *Journal of Military Communications Technology*, Vol. 32, 77–79, 2011.